



# High-pressure matrix isolation of heterogeneous condensed phase chemical reactions under extreme conditions

Jane K. Rice, T.P. Russell

*Naval Research Laboratory, Chemistry Division, Code 6110, 4555 Overlook Avenue, SW, Washington, DC 20375-5230, USA*

Received 23 September 1994; in final form 20 December 1994

---

## Abstract

A new technique which combines high-pressure and thermal-shock conditions with low-temperature matrix isolation in a gem anvil cell is presented. This serves to partially quench or arrest the reaction sequence of an energetic material. New chemical species are observed which indicate that intermediates are trapped in addition to final products. This combination of high pressure and low temperature helps elucidate the complicated reaction pathways in the deflagration to detonation regime. We have applied this technique to hexanitrohexaazaisowurtzitane (HNIW, chemical name: 2,4,6,8,10,12-hexanitro-2,4,6,8,10,12-hexaazatetracyclo[5.5.0.0<sup>5,9</sup>.0<sup>3,11</sup>]dodecane). Products are identified using infrared spectroscopy and comparisons are made to previously reported data taken under thermal, ambient pressure conditions.

---

## 1. Introduction

The study of the deflagration and detonation of energetic materials is extremely challenging due to the high-pressure, high-temperature conditions under which the chemical reactions occur. The early real-time collisional rates occur on a 1–100 ps time scale and the reactants follow on the nano- to micro-second time scale [1]. The reactions proceed through numerous pathways and yield ubiquitous final products such as H<sub>2</sub>O and CO<sub>2</sub>. The multiple phases of material present, i.e. the heterogeneous nature of the problem, and the multiple reaction pathways, both in series and parallel, make the assignment of the reaction mechanisms nearly unsolvable.

Even in the most commonly used energetic materials we know very little about the first chemical reaction steps. This knowledge would greatly reduce the possible reaction pathways. One approach has been to start with isolated molecules and study the

unimolecular bond breaking [2]. This eliminates the heterogeneous nature of the problem. Another approach is to retain the heterogeneous nature of the problem by starting with solid state material at low pressures, thus allowing the measurement of some of the stable intermediate reaction products. In this category are rapid thermolysis experiments [3,4], pyrolysis with matrix trapping [5], pyrolysis with quenching [6–8], and laser ablation with matrix isolation trapping [9]. A third approach is to imitate the pressures and temperatures of deflagration or detonation, at least initially, and detect the products formed. This approach has been used to gain information on the product sequence by initiating a detonation into a vacuum chamber and detecting the products with mass spectrometry [10].

We present a new technique in this third category, which combines high-pressure and thermal-shock conditions with low-temperature matrix isolation. This experiment is designed to model the pressures

and temperatures present in the deflagration to detonation regime. A thermally driven reaction is initiated which propagates through the material in the region of m/s to km/s. This estimate is based on studies of reaction propagation rates in a diamond anvil cell (DAC) [11]. Propagation rates up to 100 m/s were observed. The rate of propagation in the energetic material was found to depend on several parameters such as cell pressure, initial thermal shock conditions, and thermodynamic properties [11]. Similar experiments in a DAC initiated at room temperature have shown a thermally driven reaction propagating at 5–6 m/s [12]. In the experiment presented here, the reaction is partially quenched or arrested along the multiple reaction pathways by rapidly cooling the sample in the matrix as the thermal shock proceeds.

We assume the arresting occurs by trapping species in their respective potential energy wells anywhere on the multiple and branched reaction pathways. Therefore, we might expect to observe reactive as well as stable intermediates depending on how rapidly the quenching occurs. We assume that after an equilibrium temperature is established near 50 K, an ensemble of products exists representing various stages of progress toward the final reaction products. A perturbation of branching ratios in parallel pathways may occur as a result of the rapid cooling and may add complexity to the interpretation of the results.

Recent experiments [6–8] indicate that rapid quenching of chemical reactions can be used to determine the reaction dynamics of energetic materials. The early reaction mechanisms and products formed during a heterogeneous condensed phase decomposition were studied by utilizing rapid quenching. Two related techniques were employed to investigate the RDX (1,3,5-trinitro-1,3,5-triazine) condensed-phase chemistry. A thin film of RDX was deposited on a 77 K LiF salt window. During initiation with a CO<sub>2</sub> laser, the sample temperature increased at a rate of  $1 \times 10^7$  °C/s to a final temperature of  $\approx 800$  K. Calculations revealed that the sample quenched to 77 K on a millisecond time scale by the conduction of heat to the substrate. This quenching yielded early RDX decomposition products under rapid thermolysis [6,8]. In a second experiment, RDX was confined between two salt windows

to eliminate vaporization losses of the sample and products [7]. Both techniques yielded similar results for the decomposition of RDX and indicated that N–N bond cleavage was the initial dissociation step.

The value of the high-pressure matrix isolation technique presented here is demonstrated with the compound, HNIW. The HNIW molecular structure (C<sub>6</sub>H<sub>6</sub>N<sub>12</sub>O<sub>12</sub>) consists of a basic isowurtzitane cage with one NO<sub>2</sub> group appended to each of the six nitrogen atoms as shown in Fig. 1. Little or no information is available on the HNIW chemical reactions in the deflagration to detonation regime. Therefore, the data obtained under extreme conditions will be compared to the HNIW thermal decomposition [4,13–16] data at ambient pressure.

## 2. Experimental

The matrix isolation apparatus consists of a Air Products, DE-202, closed-cycle helium refrigerator (cold finger) mounted inside a vacuum chamber, a pulsed Nd:YAG laser (Quantel/Continuum, YG-581) to produce a temperature jump in the sample, and a Nicolet 60 SX FTIR spectrometer to detect the infrared active species trapped within the high-pressure matrix. A schematic of the apparatus is shown in Fig. 2.

The experiment is carried out in two stages, the initiation of the sample followed by IR spectroscopic analysis of the product. The gem anvil cell (GAC) is cooled to 50 K by thermal contact with the cold finger prior to initiation. Following initiation, the heat introduced from the laser and that generated by the deflagration are rapidly cooled by thermal conduction to the GAC. Once equilibrated, the cold steady state of the sample can be maintained indefi-

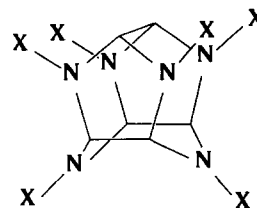


Fig. 1. A diagram of the caged molecular structure of HNIW where 'X' denotes NO<sub>2</sub>.

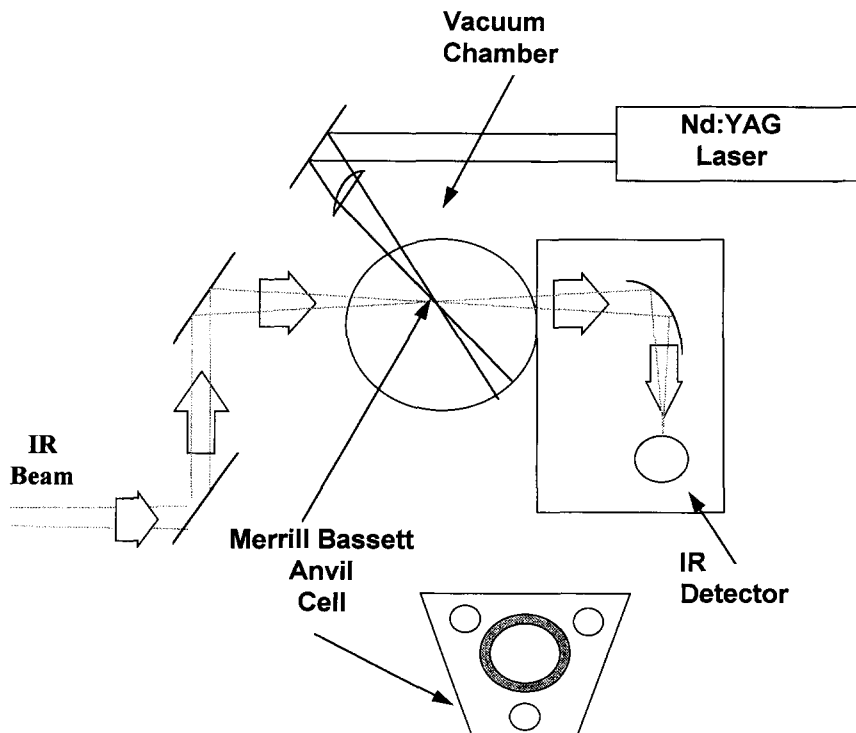


Fig. 2. Experimental setup for high-pressure matrix isolation of heterogeneous condensed phase chemical reaction under extreme conditions. Samples were initiated with a single 532 nm pulse from the Nd:YAG laser and products observed using IR spectroscopy.

nately. In the second stage, analysis of the products is achieved using IR spectroscopy. Spectra are collected at 50 K, at room temperature, and after releasing the GAC pressure. These are compared to a spectrum taken prior to the initiation of the energetic material.

The GAC is prepared by compressing a 3–5  $\mu\text{m}$  thick sample of HNIW between two KBr salt windows surrounded by a gasket as shown in Fig. 3. Typical sample masses are  $\approx 0.5\text{--}1\ \mu\text{g}$ . The gasket hole diameter is 250  $\mu\text{m}$  with a 200  $\mu\text{m}$  thickness. A small ruby sphere,  $< 15\ \mu\text{m}$ , is placed within the salt window. The combined sample (KBr salt windows and HNIW) is compressed in the GAC to the desired initial pressure. The GAC is a miniature Merrill-Basset cell fabricated from 301 stainless steel and is designed for  $180^\circ$  transmission and reflection measurements [17]. Two anvil materials, cubic zirconia (CZ) and diamond (DIA), are used to provide full spectral analysis of the mid-infrared region. CZ transmits from 4000 to 1500  $\text{cm}^{-1}$  and DIA trans-

mits from 4000 to 2300 and from 1500 to 600  $\text{cm}^{-1}$ . Separate samples are loaded with CZ and DIA anvils. Each anvil material provides a maximum pressure in excess of 10.0 GPa [18]. Pressure inside the anvil cell is measured by the ruby fluorescence pressure

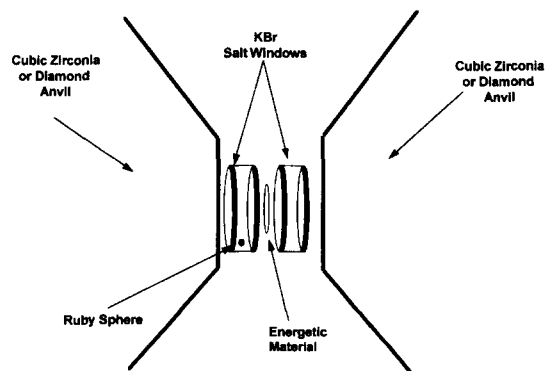


Fig. 3. Sample arrangement inside the Merrill-Basset gem anvil cell. The sample is surrounded by a metal gasket not represented in the figure.

measurement technique [19,20] and calibrated against the compression of NaCl via the Decker equation of state [21]. Pressure is evaluated by a peak shift calculation or a line-shape model. The ruby fluorescence measurements are accurate to  $\pm 0.05$  GPa when they are made in a hydrostatic environment at room temperature. The uncertainty is  $\pm 0.15$  GPa in KBr due to the absence of strictly hydrostatic conditions. The cell is mounted in thermal contact with the cold finger and is cooled to a constant temperature of 40–50 K. The temperature is measured with two gold/chromel thermocouples. One thermocouple is located in a drilled hole in an aluminum mounting plate between the cold finger and the anvil cell. The second is attached to the gasket surrounding the sample.

A single flash (8 ns) from the Nd:YAG laser (532 nm) is selected to heat the sample. The typical laser energies delivered to the sample are  $\approx 10$  mJ. The laser beam diameters are determined separately by measuring the spot size burned onto photographic paper loaded in the GAC. Typical values for the beam diameters are  $\approx 0.5$  mm. The laser fluence is  $\approx 5$  J/cm<sup>2</sup>. Under these conditions, an initial temperature between 300 and 740°C (573 and 1013 K) is obtained within the sample. The lower temperature is the minimum required to thermally decompose  $\zeta$ -HNIW at this pressure [22]. The higher temperature is the melting temperature of KBr, which we do not exceed. In the experiments with DIA, we have burned the surface of the DIA anvil with the laser initiation pulse. The burning or combustion of DIA occurs at 600°C or 873 K, placing a stricter limitation on the lower temperature.

The background pressure of the chamber is typically  $\approx 1 \times 10^{-7}$  Torr. The sample pressure inside the anvil cell is  $\approx 2.7$  GPa. Vacuum conditions are required to obtain the cooling of the cold finger and GAC to  $\approx 50$  K with minimal conduction losses.

Infrared absorption spectra of the starting material and the reaction products are measured before and after the laser pulse. The infrared beam is directed externally from the FTIR bench and is focused through the anvil cell mounted inside the vacuum chamber using a series of mirrors and a 250 mm f.l. ZnSe lens. The transmitted infrared signal is recollimated through a second 250 mm f.l. lens and focused onto an externally mounted MCT-A detector

using a series of mirrors. Spectra are collected with 2000–10000 scans at 2 cm<sup>-1</sup> resolution.

The HNIW samples were supplied by W. Koppess and are used without further purification. Five HNIW polymorphs ( $\alpha$ ,  $\beta$ ,  $\gamma$ ,  $\epsilon$  and  $\zeta$ ) have been identified and confirmed by single crystal X-ray diffraction and infrared spectroscopy [14,22,23]. In the experiments presented here,  $\gamma$ -HNIW is loaded into the GAC and is transformed to  $\zeta$ -HNIW when pressurized to 2.7 GPa [22,23].

### 3. Results

Figs. 4 and 5 show selected spectra of the laser initiation results of  $\zeta$ -HNIW in a cubic zirconia anvil cell (CZAC) and a DAC, respectively. Fig. 4A shows the infrared spectra at 50 K and 2.7 GPa prior to laser initiation. Fig. 4B show the infrared spectra of the reaction products formed after laser initiation, i.e. after the arrested reaction of  $\zeta$ -HNIW in the deflagration to detonation regime. No starting material remains, indicating that the reactant is completely consumed. Fig. 5A shows the reaction products formed after laser initiation in the DAC. Fig. 5B shows the room temperature spectrum of the warmed products. Fig. 5C shows the atmospheric pressure spectrum of the products, i.e. the residue. Comparison of the overlapping wavenumber regions in Figs. 4B and 5A indicate that similar products are observed in the CZAC and DAC at 2.7 GPa and 50 K.

The products formed are identified by their infrared absorption frequencies. The tentative assignments for the reaction products are shown in Table 1. The products observed at 50 K, including unknown (Unk) absorption bands are: CO<sub>2</sub>, Unk 3117, Unk 3040, H<sub>2</sub>O, Unk 1413, NO<sub>2</sub>, CO, HNCO, Unk 2813, *t*-(NO)<sub>2</sub>, Unk 2015, and N<sub>2</sub>O. These are listed roughly in order of their peak height intensity in the spectra without linestrength corrections. The peak heights from the DAC are multiplied by three to scale them roughly to that of the CZAC data. The three unknown absorption bands at 3117, 3040, and 1413 cm<sup>-1</sup> are tentatively assigned to the formation of at least one product containing NH functionality. Two additional absorption bands are detected at 2813 and 2015 cm<sup>-1</sup> which are tentatively assigned to at least one product containing CH and CN. Several

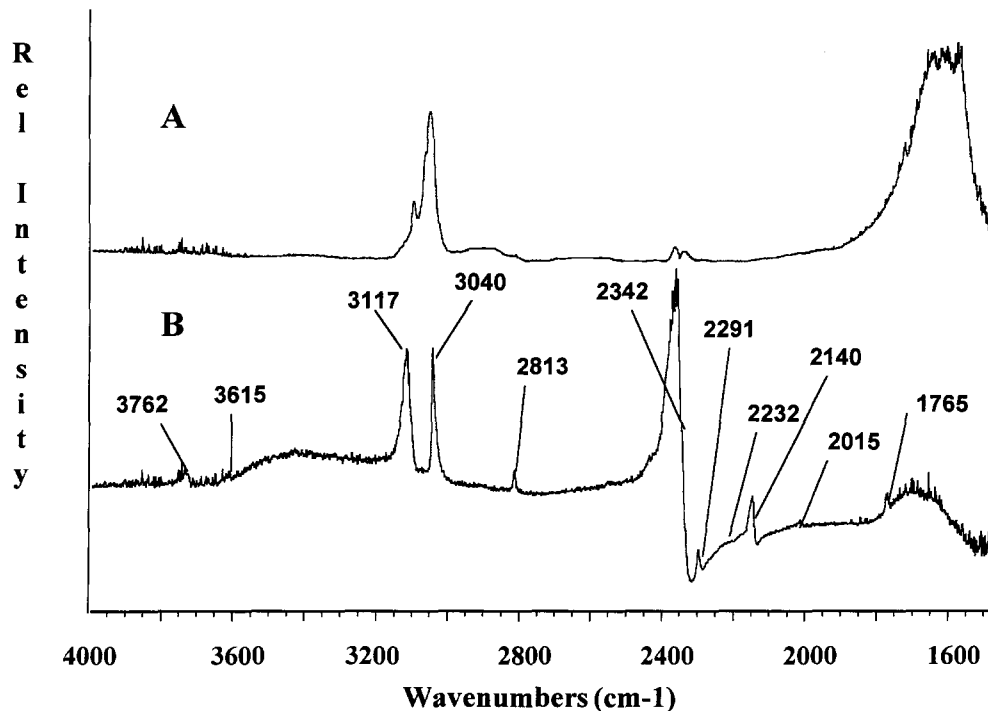


Fig. 4. These spectra are taken in a cubic zirconia anvil cell. A spectrum of  $\zeta$ -HNIW at 2.7 GPa and  $\approx 50$  K before laser heating is shown in (A). The products from HNIW at 2.7 GPa and  $\approx 50$  K after laser heating are shown in (B). Frequencies and tentative assignments are given in Table 1.

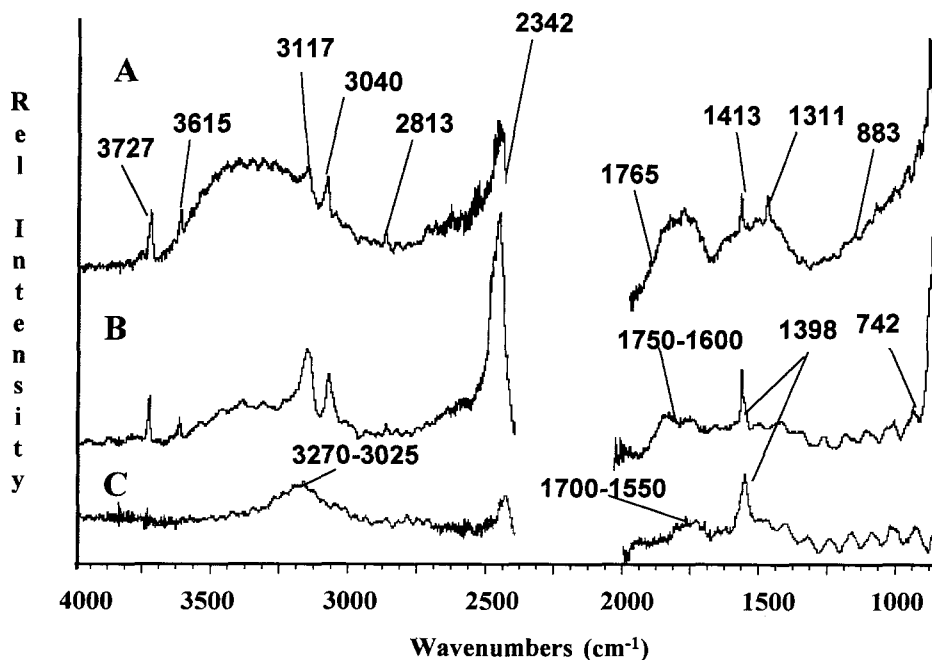


Fig. 5. These spectra are taken in a diamond anvil cell. A spectrum of  $\zeta$ -HNIW at 2.7 GPa and  $\approx 50$  K following laser initiation is shown in (A). Spectrum (B) is taken after warming to room temperature. Spectrum (C) is the residue of (B) after pressure is released to 1 atm. Frequencies and tentative assignments are given in Tables 1 and 2.

Table 1

IR bands and tentative assignments of the observed products from reacted  $\zeta$ -HNIW in cubic-zirconia (OZ) and diamond (DIA) anvil cells

$\nu$ ( $\text{cm}^{-1}$ )	Species	Tentative assignment (intensity)	In CZ <sup>c</sup>	In DIA <sup>c</sup>
3727	CO <sub>2</sub> or H <sub>2</sub> O	$\nu_1 + \nu_3(39)$ or $\nu_3(200)$	Y	Y
3615	CO <sub>2</sub> or HOCN(?)	$2\nu + \nu_3(30)$ or OH str	Y	Y
≈ 3600 (broad)	H <sub>2</sub> O	OH str	Y	Y
3117	–NH <sup>a</sup> or –CH	NH str or CH str	Y	Y
3040	–NH <sup>a</sup> , –CH or –CH <sub>2</sub>	NH str or CH str	Y	Y
2813	–CH or –CH <sub>2</sub>	CH str	Y	Y
2342	CO <sub>2</sub>	$\nu_3(2026)$	Y	Y (edge)
2291	HNCO or HOCN	NCO a-str or CN str	Y	
2232	N <sub>2</sub> O	$\nu_3(1285)$	Y	
2140	CO	1–0 (235)	Y	
2015	–CH or –CN(?)		Y	
1765	<i>t</i> -(NO) <sub>2</sub>	a-str	Y	Y
1413	–NH <sup>a</sup> or HNO(?) or CH <sub>3</sub> NO(?) or H <sub>2</sub> CN(?)	NO str CH <sub>3</sub> a-def CH <sub>2</sub> sciss		Y
1311	NO <sub>2</sub> (?) <sup>b</sup>	s-str <sup>b</sup>		Y
883	–CH(?) or –CH <sub>2</sub> (?)	CH or CH <sub>2</sub> bend(?)		Y
742	–CH(?)			Y
≈ 650	CO <sub>2</sub>	$\nu_2^1(194)$		Y

<sup>a</sup> Similar to HN<sub>3</sub> decomposition products in Refs. [26,27]. <sup>b</sup> Not seen in post-laser fire room temperature spectrum.<sup>c</sup> The 'Y' represents 'yes', the band was observed in the corresponding GAC material.

products containing individual or multiple NH, CH and CN functionality have been observed in uni-molecular dissociation experiments [24], although the physical conditions were significantly different.

As the sample is warmed to room temperature the *t*-(NO)<sub>2</sub> band observed at 1765 cm<sup>-1</sup> disappears and a band at 1873 cm<sup>-1</sup> appears. This is shown in Fig. 5B. The 1873 cm<sup>-1</sup> absorption is attributed to the NO monomer and the conversion between monomer and dimer is reversible. A band at 1311 cm<sup>-1</sup> which is evident in the 50 K spectrum also disappears at room temperature. This has been tentatively assigned to the symmetric stretch of NO<sub>2</sub>. It is not observed

Table 2

IR bands and tentative assignments of the observed products from the residue

$\nu$ ( $\text{cm}^{-1}$ )	Species	Tentative assignment
3270–3025	–NH(?)	–NH str
1700–1550	–C=O, –CN, –NO <sub>2</sub> , H <sub>2</sub> O	
1398	–C–NO <sub>2</sub>	–NO str

in the room temperature spectrum, but may become allowed through distortions under the high-pressure/low-temperature conditions. This is also a reversible process. No other changes are observed when the sample is warmed to room temperature.

After the pressure is decreased from 2.7 GPa to atmospheric pressure (Fig. 5C) the reaction products observed at 50 K and room temperature disappear. These products are either volatile or reactive intermediates. The only remaining absorptions correspond to the IR spectrum of a dark residue film trapped in the salt matrix. The residue spectrum is similar but not identical to the  $\gamma$ -HNIW decomposition residue previously reported [13,15]. Tentative assignments for the observed IR bands of the residue are given in Table 2.

#### 4. Discussion

Prior to this study, the decomposition/deflagration chemistry of HNIW was investigated using a variety of thermolysis techniques [4,13–16]. All

measurements were made on the  $\gamma$  polymorph. Under these thermolysis conditions, the products identified were  $\text{NO}_2$ ,  $\text{CO}_2$ ,  $\text{N}_2\text{O}$ ,  $\text{NO}$ ,  $\text{CO}$ ,  $\text{HCN}$ ,  $\text{H}_2\text{O}$ ,  $\text{HNCO}$  and a polymer residue with a molecular composition of  $\text{C}_4\text{H}_4\text{N}_4\text{O}_2$ . Using the populations reported [4] and the proper linestrengths<sup>1</sup> we can estimate the relative intensities of their major species:  $\text{NO}_2(40)$ ,  $\text{CO}_2(4.3)$ ,  $\text{N}_2\text{O}(4.0)$ ,  $\text{NO}(2.0)$ ,  $\text{HCN}(1.0)$  and  $\text{CO}(1.0)$ . The populations of  $\text{H}_2\text{O}$  and  $\text{HNCO}$  were not quantified [4].

High-pressure matrix isolation of the reaction of  $\zeta$ -HNIW in the deflagration to detonation regime has detected significant differences in products observed when compared to thermolysis results. A crude estimate of our relative intensities from the peak heights of identified bands is  $\text{CO}_2(27)$ ,  $\text{NO}_2(7)$ ,  $\text{CO}(5)$ ,  $\text{HNCO}(3)$  and  $t\text{-(NO)}_2(1-3)$ . We have arbitrarily scaled the weakest bands in both sets of data to be  $\approx 1$  in relative intensity. Only a very small quantity of  $\text{NO}_2$  is observed under our conditions.  $\text{NO}_2$  is reported to be the major decomposition product under rapid heating ( $2000^\circ\text{C/s}$ ) and atmospheric pressure [4] and is believed to result from N–N homolysis. The small amount of  $\text{NO}_2$  observed in high-pressure matrix isolation is probably not due to an initial N–N homolysis reaction. Furthermore, several new unidentified product absorptions are detected at 3117, 3040, 2813, 2015, and  $1413\text{ cm}^{-1}$ . These absorption are tentatively assigned in Table 1 to products with NH, CH and CN functionality.

The residue spectrum shown in Fig. 5C is similar to that of the thermolysis experiments with the exception of one new broad band which appears at  $1398\text{ cm}^{-1}$ . This is tentatively assigned as a C– $\text{NO}_2$  stretching mode. During thermal decomposition of the  $\gamma$ -HNIW residue,  $\text{HCN}$  and  $\text{HNCO}$  were observed as the major decomposition products [13]. We do not observe  $\text{HCN}$  during the reaction of  $\zeta$ -HNIW, indicating that our residue does not reach the fully deflagrated/detonated final products.

If quenching due to low temperature and high pressure is arresting reactions at a variety of steps

along the deflagration to detonation process, as we believe, it is the effect of pressure (2.7 GPa) which retains that state after the sample is warmed. This may be due to the formation of solidous or liquidous products at 2.7 GPa which are much less reactive than their gaseous counterparts at 1 atm. Prior to these experiments, energetic materials were initiated in a CZAC cell at room temperature. However, with no cooling of the sample the energy released from materials less energetic than HNIW (ADN and RDX) was large enough to break and sometimes pulverize the anvils.

Because the observed products are significantly different than those seen in any other thermal or laser-initiated study, we conclude the chemical pathways or the extent of completion of the pathways is qualitatively different. Based on our rapid cooling conditions and our previous experience with laser initiation at room temperature, we propose this is due to an arresting of the reaction. A more precise assignment of several of the new reaction products will be determined through isotopic substitution studies.

## 5. Conclusion

High-pressure matrix isolation has been first demonstrated and shown to be a valuable technique for studying product formation in the heterogeneous condensed phase chemistry of materials under extreme conditions. We have applied this technique to the study of the  $\zeta$ -HNIW reaction. From this we have tentatively assigned a variety of products:  $\text{CO}_2$ ,  $\text{H}_2\text{O}$ ,  $\text{NO}_2$ ,  $\text{CO}$ ,  $\text{HNCO}$ ,  $t\text{-(NO)}_2$  and  $\text{N}_2\text{O}$ . Five new, unidentified infrared absorption bands at 3117, 3040, 2813, 2015 and  $1413\text{ cm}^{-1}$  have been observed. The 3117, 3040 and  $1413\text{ cm}^{-1}$  are tentatively assigned to one or more –NH species. The 2813 and  $2015\text{ cm}^{-1}$  are tentatively assigned to be at least one –CH and –CN species. The new products detected from the isolation of  $\zeta$ -HNIW reactions in the deflagration to detonation regime are either reactive intermediates or volatile products. The residue spectrum is similar but not identical to that reported previously [13,15]. We observe an additional residue feature at  $1398\text{ cm}^{-1}$ , tentatively identified as a C– $\text{NO}_2$  stretching mode. Based on this new information, we believe the combination of high pressure

<sup>1</sup> The values taken from the table in Ref. [25] are  $\text{CO}_2 = 2580\text{ cm}^{-2}\text{ atm}^{-1}$  at  $2349\text{ cm}^{-1}$ ;  $\text{N}_2\text{O} = 1421$  at  $2224$ ;  $\text{NO}_2 = 1419$  at  $1621$ ;  $\text{CO} = 268$  at  $2145$ ;  $\text{HCN} = 260$  at  $713$ ; and  $\text{NO} = 133$  at  $1876$ .

and low temperature arrests the reaction before it proceeds to completion.

### Acknowledgements

The authors wish to gratefully acknowledge financial support from the Office of Naval Research and Naval Research Laboratory accelerated research initiative on the heterogeneous decomposition of energetic materials.

### References

- [1] A. Tokmakoff, M.D. Fayer and D.D. Dlott, *J. Phys. Chem.* 97 (1993) 1901.
- [2] X. Zhao, E.H. Hintsa and Y.T. Lee, *J. Chem. Phys.* 88 (1988) 801.
- [3] T.B. Brill and K. James, *Chem. Rev.* 93 (1993) 2667.
- [4] D.G. Patil and T.B. Brill, *Combustion Flame* 87 (1991) 145.
- [5] M.J. Rossi, J.C. Bottaro and D.F. McMillen, *Intern. J. Chem. Kinetics* 25 (1993) 549.
- [6] C.A. Wight and T.R. Botcher, *J. Am. Chem. Soc.* 114 (1992) 8303.
- [7] T.R. Botcher and C.A. Wight, *J. Phys. Chem.* 97 (1993) 9149.
- [8] T.R. Botcher and C.A. Wight, *J. Phys. Chem.* 98 (1994) 5441.
- [9] L. Pasternack and J.K. Rice, *J. Phys. Chem.* 97 (1993) 12805.
- [10] N.C. Blais, *J. Energ. Mat.* 6 (1987) 255.
- [11] S.F. Rice and M.F. Foltz, *Combustion Flame* 87 (1991) 107.
- [12] T.P. Russell, T.M. Allen, J.K. Rice and Y.M. Gupta, *J. Phys. (Paris)*, in press.
- [13] D.G. Patil and T.B. Brill, *Combustion Flame* 92 (1993) 456.
- [14] K.J. Kraeutle, *JANNAF Proc.*, CPIA publication No. 498, October 1988.
- [15] K.J. Kraeutle, *JANNAF Proc.*, CPIA publication No. 557, 1990, Vol. III, p. 259.
- [16] R.Y. Yee, M.P. Nadler, A.T. Neilson, *JANNAF Proc.*, CPIA publication, October 1990.
- [17] L. Merrill, and W.A. Bassett, *Rev. Sci. Instr.* 45 (1974) 290.
- [18] T.P. Russell and G.J. Piermarini, unpublished result.
- [19] J.D. Barnett, S. Block and G.J. Piermarini, *Rev. Sci. Instr.* 44 (1973) 1.
- [20] S. Block and G.J. Piermarini, *Phys. Today* 29 (1976) 44.
- [21] G.J. Piermarini, S. Block, J.D. Barnett and R.A. Forman, *J. Appl. Phys.* 46 (1975) 2774.
- [22] T.P. Russell, P.J. Miller, G.J. Piermarini and S. Block, *J. Phys. Chem.* 97 (1993) 1993.
- [23] T.P. Russell, P.J. Miller, G.J. Piermarini and S. Block, *J. Phys. Chem.* 96 (1992) 5509.
- [24] R.J. Doyle Jr., *Organic Mass Spectry.* 26 (1991) 723.
- [25] Y. Oyumi and T.B. Brill, *Combustion Flame* 62 (1985) 213.
- [26] E.J. Blau and B.F. Hochheimer, *J. Chem. Phys.* 34 (1961) 1060.
- [27] E.J. Blau and B.F. Hochheimer, *J. Chem. Phys.* 41 (1964) 1174.